Gene Expression of Osteosarcoma Cells on Various Coated Titanium Materials

Sung-Hwa Sohn[1], **Jae Bun Lee**[2], **Ki-Nam Kim**[1],
In Kyoung Kim[1], **Seung Ho Lee**[1], **Hye Won Kim**[1],
Sang-Hui Seo[1], **Yu-Ri Kim**[1], **Sang-Wan Shin**[2],
Jae-Jun Ryu[2] **& Meyoung-Kon Kim**[1]

[1]Department of Biochemistry & Molecular Biology
[2]Department of Dentistry, College of Medicine, Korea University,
Seoul 136-705, Korea
Correspondence and requests for materials should be addressed
to M-K. Kim (jerrykim@korea.ac.kr)

Abstract

Several features of the implant surface, such as topography, roughness, and composition play a relevant role in implant integration with bone. This study was conducted in order to determine the effects of different-coatings on Ti surfaces on the biological responses of a human osteoblast-like cell line (MG63). MG63 cells were cultured on HA (Hydroxyapatite coating on Titanium), Ano (HA coating on anodized surface Titanium), Zr (zirconium-coating on Titanium), and control (non-coating on Titanium). The morphology of these cells was assessed by SEM. The cDNAs prepared from the total RNAs of the MG63 were hybridized into a human cDNA microarray (1,152 elements). The appearances of the surfaces observed by SEM were different on each of the three dental substrate types. MG63 cells cultured on HA, Ano, Zr, and control exhibited cell-matrix interactions. In the expression of several genes were up-, and down-regulated on the different surfaces. The attachment and expression of key osteogenic regulatory genes were enhanced by the surface morphology of the dental materials used.

Keywords: Titanium, HA coating, Gene expression profiling, cDNA microarray

Titanium (Ti) and its alloys have been widely used for implants that interact with bone cells *in vitro* and *in vivo*[1]. For decades, maxillofacial, and orthopedic surgeons have placed implants, screws and plates, and prostheses to substitute lost teeth, to fix bone fragments, and to replace joints, respectively. Als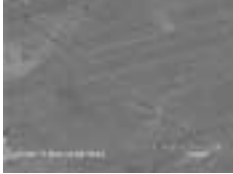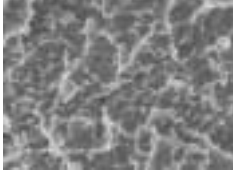o, many surgical instruments, such as drills and saws, are made with Ti alloys. However, the exact effect of Ti on osteoblasts is still unknown[2-4]. Successful application of such materials for bone regeneration often involved mixing with autogenous bone, a source of osteoblastic cells and precursors[2].

Surface topography may affect the formation of a fibrous capsule around implants, inflammatory response at tissue-implant interface, fibroblast attachment, angiogenesis, epithelial down-growth around percutaneous devices, and many cellular processes such as cellular differentiation, transcription, cell metabolism, protein production, and phenotypic expression[1,3,5-7]. Diverse implant surface may contribute to the regulation of osteoblast differentiation by influencing the level of gene expression of key osteogenic factors[7,8]. Morphometric analyses had shown differences in bone-implant contact percentages with the varying of surface characteristics, as well as a sensitivity of cells to surface topography[9,10]. Gene expression in response to the placement of implants with different surface topographies[11-16]. Biomaterial composition and surface topography regulate cell attachment, focal contact formation and cytoskeletal organization with long-term effects on osteoblastic cell maturation, and subsequent mineralization[17].

We hypothesized that different-coatings on Ti surface conditions would be associated with differential bone-matrix gene expression and interfacial strengths, which may lead to the development of more advanced therapeutic prosthetic interventions associated with dental implant therapy and tissue-engineering biological applications.

Scanning electron microscopic (SEM) examinations revealed morphologic differences on Ti surfaces (Table 1). Figure 1 is scatter plot for comparing the expression profiles of different-coatings on Ti and control. Regeneration analysis of Z scores from two independent samples of different ceramic-coatings on Ti and control were performed and Z scores of individual genes were plotted. To obtain a molecular portrait of the relationships between the metabolisms associated with experimental group, we used a hierarchical clustering algorithm to group genes on the basis of similar expression patterns and the data is presented in a matrix format (Figure 2). Each row of Figure 2 represents the hybridization results for a single DNA element of the array and each column represents the expression levels for all genes in a

Table 1. The surface morphology & characteristics.

	Coating	Surface morphology
Control	Non-coating on Titanium	
HA	HA coating on Titanium	
ANO	HA coating on anodized surface Titamium	
Zr	Zrconium coating on Titanium	

*Magnification 3000×, Ti surface morphology using a scanning electron microscopy (SEM).

single hybridization sample. The expression level of each gene was visualized in color, relative to its median expression level across all samples. Red represented expression greater than the mean, green represents expression less than the mean and color intensity denotes the degree of deviation from the mean. Gray represented the median expression level. Distinct samples representing similar gene patterns from control cells were aligned in adjacent rows. The cells included in this map were samples from right experimental and control group. Coordinately expressed genes were grouped into clusters, which were named on the basis of the cellular process in which the component genes participated in. The clustergram revealed that clusters of genes related to progression were up- and down-regulated in experimental group, as compared to control group (Figure 2). Table 2 shows the expression of various genes in different Ti surfaces compared with the control group.

Discussion
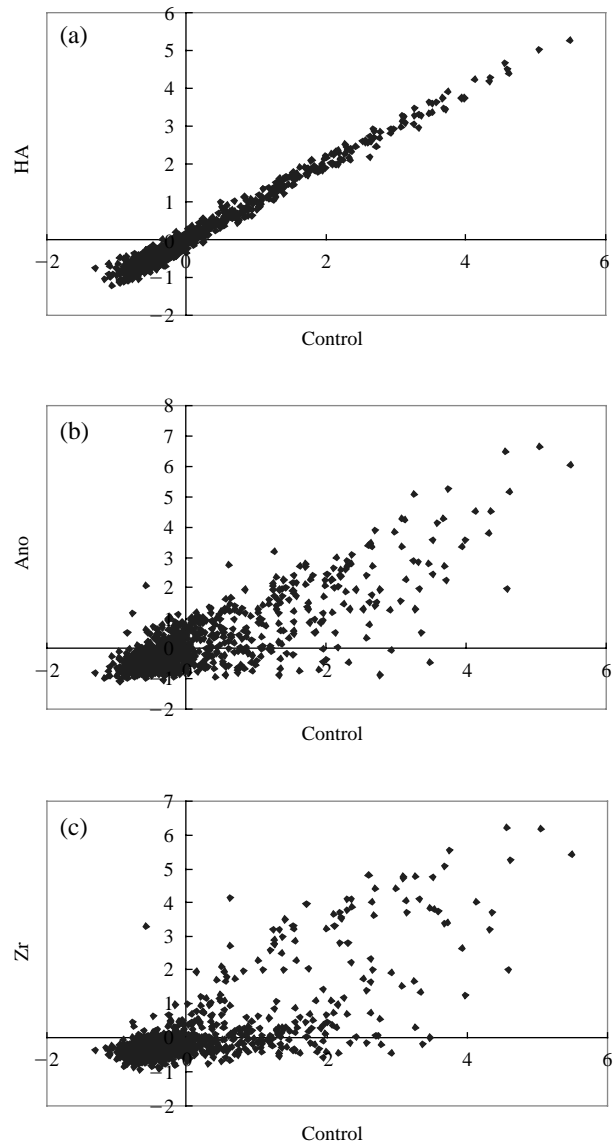
The frequently observed unwanted biological

Figure 1. Scatter plots for comparison of expression profile between control and different coating on Ti surface. Expression profiles of control (Non-coating on Titanium) versus different coating on Ti surface on MG63 cells. (a) HA (Hydroxyapatite coating on Titanium) on MG63 cells versus control; (b) Ano (HA coating on anodized surface Titamium) on MG63 cells versus control; (c) Zr (Zrconium coating on Titanium) on MG63 cells versus control are shown as bivariate scatter plots of 1,152 genes from the microarray. The values are corrected intensities relative to control, representing levels of expression for the DNA elements of the microarrays.

effects of different metals require *in vitro* and *in vivo* biological tests of any medical or dental device before its definite use in humans. Biological testing of medical and dental devices is necessary in order to
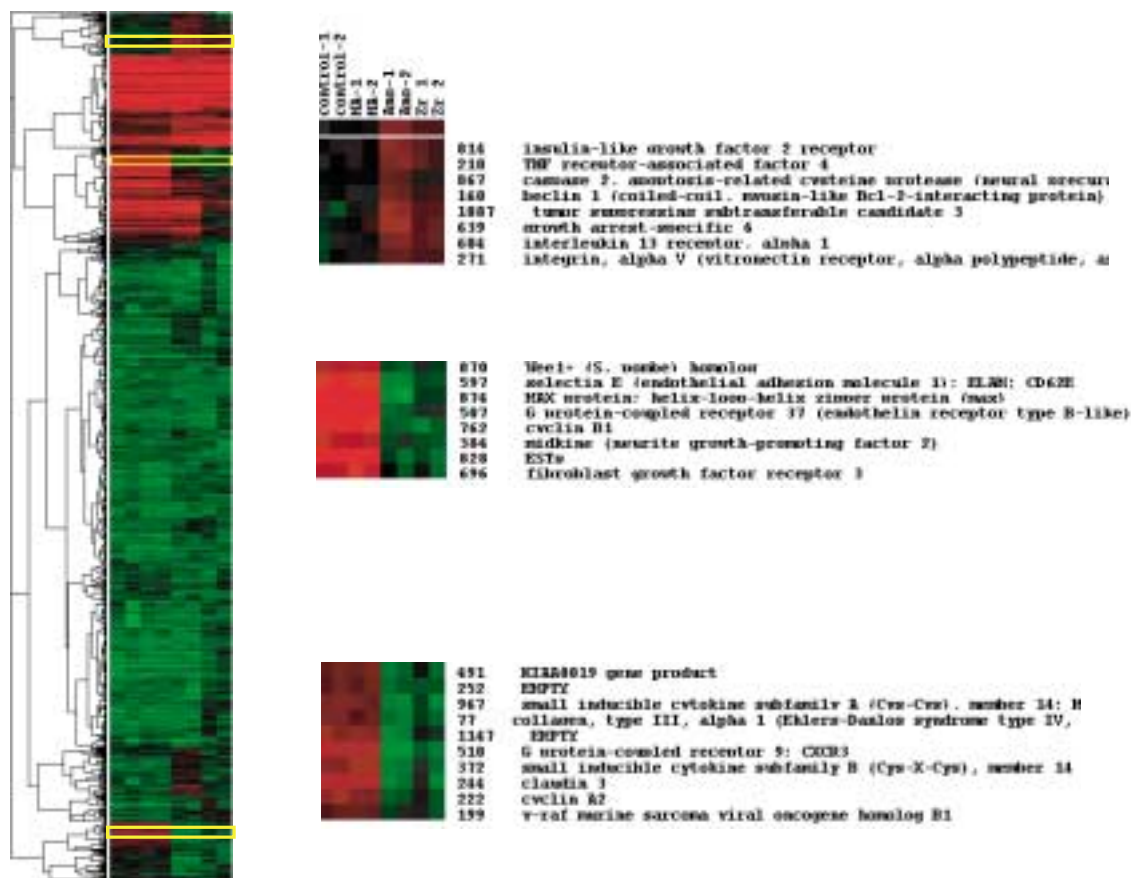
Figure 2. Molecular portrait of different Ti surfaces on MG63 cells. Cells were treated with different Ti for 72 h. Microarray data from controls (Non-coating on Titanium) and HA (Hydroxyapatite coating on Titanium), Ano (HA coating on anodized surface Titamium), or Zr (Zrconium coating on Titanium) treated cells were combined and clustered. Cluster analysis was performed on Z-transformed microarray data using two separate programs available as shareware from Michael Eisens' lab. Each gene is represented by a single row of colored boxes; each experimental sample is represented by a single column. The entire clustered image is shown on the left. Full gene names are shown for coordinately expressed clusters, containing genes involved in osteointegration.

evaluate the biological behaviour of biomaterials. Osteoblastic cells began to secrete several extracellular matrix (ECM) proteins. They will also attach on the implant surface and are necessary for adhesion due to their specific binding to cell surface receptors. The formation of cell attachment to the alloys seems to be slower than on pure Ti. A reasonable explanation for this observation is that the formation of cell-implant contacts may be hampered on rough surfaces[18,19] while Carinci *et al.*[20] and Lossdorfer *et al.*[21] demonstrated that surface roughness affects proliferation, differentiation, local factor production. And alkaline phosphatase, osteocalcin, and Transforming Growth Factor beta were increased on the rougher surfaces. We also attempted to determine the effects of different implant surfaces on the phenotype and gene expression of MG63 cells. In the experimental

cultures, several genes were up-regulated or down-regulated (Figure 2). These genes were categorized depending on their functions, as follows (Table 2).

The bone morphogenetic proteins (BMPs) are a family of secreted signaling molecules that can induce ectopic bone growth. Many BMPs are part of the transforming growth factor-beta (TGFB) superfamily. BMPs were originally identified by an ability of demineralized bone extract to induce endochondral osteogenesis *in vivo* in an extraskeletal site. Based on its expression early in embryogenesis, the BMP encoded by this gene has a proposed role in early development. In addition, the fact that this BMP is closely related to BMP5 and BMP7 has led to speculation of possible bone inductive activity[22,23]. In our experiment, we noted the up-regulation of BMP8 and BMPR2 on HA surfaces, and an up-regulation of

Table 2. Up-and down-regulated Genes of MG63 on different-coated Ti surface.

Genes	Abb.	Regulation profile and Z-ratio		
		HA	ANO	Zr
interferon regulatory factor 7C	IRF7	**3.96**	0.81	1.35
transforming growth factor, beta receptor II (70-80 kD)	TGFBR2	**3.48**	0.77	1.13
cyclophilin-like protein	CYLP	**3.39**	0.97	0.53
microsomal glutathione S-transferase 2	MGST2	**3.35**	0.61	1.09
bone morphogenetic protein 8 (osteogenic protein 2)	BMP8	**2.94**	0.82	0.81
protein tyrosine phosphatase	PTP	**2.82**	0.81	0.85
cyclophilin	USA-CYP	**2.78**	0.48	0.43
requiem, apoptosis response zinc finger gene	REQ	**2.57**	0.57	−0.39
GCN1 (general control of amino-acid synthesis, yeast, homolog)-like	GCN1	**2.55**	0.62	0.67
proteasome (prosome, macropain) subunit, alpha type, 2	PSMA2	**2.49**	1.20	**2.28**
v-maf musculoaponeurotic fibrosarcoma (avian) oncogene homolog	MAF	**2.47**	−0.13	0.59
core-binding factor, beta subunit	CBFB	**2.40**	1.24	1.73
BMPR-II precursor; bone morphogenetic protein type II receptor	BMPR2	**2.35**	1.20	1.51
ubiquitin-conjugating enzyme E2A (RAD6 homolog)	UBE2A	**2.30**	0.59	0.14
tumor protein p53-binding protein	TP53BPL	**2.29**	1.09	0.70
brain-derived neurotrophic factor	BDNF	**2.29**	1.02	0.72
sterile 20 (oxidant stress response kinase 1; yeast Sps1/Ste20-related kinase 1)	YSK1	**2.22**	1.10	0.43
GTP-binding protein Ran/TC4	RAN	**2.21**	0.23	0.08
small inducible cytokine subfamily B (Cys-X-Cys), member 14 (BRAK)	SCYB14	**2.18**	**−2.53**	−1.64
interferon (alpha, beta and omega) receptor 1	IFNAR1	**2.17**	0.80	**−2.12**
deoxyribonuclease II, lysosomal	DNASE2	**2.14**	1.04	−1.81
prostaglandin-endoperoxide synthase 2 (prostaglandin G/H synthase and cyclooxygenase)	PTGS2	**2.12**	−0.03	−0.10
tyrosine kinase 2	TYK2	**2.11**	1.00	0.37
general transcription factor IIF, polypeptide 2 (30 kD subunit)	GTF2F2	**2.09**	0.19	0.53
jun activation domain binding protein	JAB1	**2.05**	**4.48**	**5.50**
small inducible cytokine A7 (monocyte chemotactic protein 3; Mcp-3)	SCYA7	**2.01**	−0.26	0.49
Janus kinase 1 (a protein tyrosine kinase)	JAK1	**2.00**	0.11	0.81
upstream transcription factor 2, c-fos interacting	USF2	**−3.00**	**−3.12**	**−2.68**
tumor necrosis factor receptor superfamily, member 6; apoptosis (APO-1) antigen 1	TNFRSF6	**−2.74**	−0.62	−0.04
cytochrome c oxidase subunit VIIc	COX7C	**−2.64**	−0.82	1.14
clusterin (complement lysis inhibitor, SP-40,40, sulfated glycoprotein 2, testosterone-repressed prostate message 2, apolipoprotein J)	CLU	**−2.62**	−0.28	0.03
paired box gene 5 (B-cell lineage specific activator protein)	PAX5	**−2.57**	0.13	0.48
coagulation factor II (thrombin) receptor	F2R	**−2.49**	−0.30	−0.15
TATA box binding protein (TBP)-associated factor, RNA polymerase II, G, 32 kD	TAF2G	**−2.44**	0.73	−0.15
forkhead (Drosophila)-like 1	FKHL1	**−2.44**	0.14	0.18
v-src avian sarcoma (Schmidt-Ruppin A-2) viral oncogene homolog	SRC	**−2.37**	0.53	0.75
interleukin 1 receptor, type I	IL1R1	**−2.28**	0.05	0.23
integral membrane protein 2B	ITM2B	**−2.28**	−1.18	−0.98
defensin, alpha 5, Paneth cell-specific	DEFA5	**−2.25**	−0.35	0.04
mitogen-activated protein kinase 13	MAPK13	**−2.23**	−0.04	0.22
synaptophysin	SYP	**−2.17**	−0.67	0.16
mitogen-activated protein kinase kinase 1	MAP2K1	**−2.07**	−0.84	−0.38
interleukin enhancer binding factor 1	ILF1	**−2.04**	0.18	0.43
proteasome (prosome, macropain) subunit, alpha type, 1	PSMA1	0.29	**3.61**	**5.03**
caspase 1, apoptosis-related cysteine protease (interleukin 1, beta, convertase)	CASP1	0.93	**3.25**	**2.18**
Bruton agammaglobulinemia tyrosine kinase	BTK	0.77	**3.21**	**2.35**
adrenergic, beta-2-, receptor, surface	ADRB2	−1.91	**3.21**	1.75
singed (Drosophila)-like (sea urchin fascin homolog like)	SNL	0.20	**3.04**	**2.18**
thyroid stimulating hormone receptor	TSHR	−0.23	**2.68**	1.60
chemokine (C-C motif) receptor 5	CCR5	1.05	**2.51**	**2.55**
frataxin; Friedreich ataxia	FRDA	0.65	**2.26**	0.98
tumor suppressing subtransferable candidate 3	TSSC3	1.78	**2.09**	0.98

Table 2. Continued.

Genes	Abb.	Regulation profile and Z-ratio		
		HA	ANO	Zr
growth arrest-specific 6	GAS6	1.86	**2.08**	0.85
farnesyl-diphosphate farnesyltransferase 1	FDFT1	1.05	**2.04**	0.88
Bcl-2-like 11 (apoptosis facilitator)	BCL2L11	0.64	**2.04**	1.06
EphB3	EPHB3	0.04	**2.04**	**2.46**
DNA (cytosine-5-) methyltransferase 3 beta	DNMT3B	1.29	**2.00**	**2.33**
amyloid beta (A4) precursor protein (protease nexin-II)	APP	1.09	**−6.65**	**−4.94**
MAX protein; helix-loop-helix zipper protein (max)	MAX	0.53	**−6.15**	**−4.24**
fibroblast growth factor 12	FGF12	−0.05	**−5.05**	**−4.80**
retinoblastoma-like 1 (p107)	RBL1	−0.61	**−4.80**	**−5.02**
G protein-coupled receptor 37 (endothelin receptor type B-like)	GPR37	−1.12	**−4.70**	**−3.51**
synuclein, alpha (non A4 component of amyloid precursor)	SNCA	−0.64	**−4.42**	**−3.67**
selectin E (endothelial adhesion molecule 1); ELAM; CD62E	SELE	−0.75	**−4.39**	**−3.15**
cyclin B1	CCNB1	−0.14	**−4.02**	**−3.61**
MAD (mothers against decapentaplegic, Drosophila) homolog 5	MADH5	0.28	**−3.76**	**−3.87**
G protein-coupled receptor 9; CXCR3	GPR9	−0.16	**−3.71**	**−2.66**
TCR adaptor molecule cbl-b	CBLB	−1.22	**−3.57**	**−3.71**
claudin 3	CLDN3	−0.17	**−3.42**	**−2.35**
interleukin 12B	IL12B	−0.89	**−3.31**	**−2.89**
breast cancer 1, early onset	BRCA1	1.45	**−3.30**	**−4.22**
midkine (neurite growth-promoting factor 2)	MDK	−0.73	**−2.91**	**−2.67**
Wee1+ (S. pombe) homolog	WEE1	0.61	**−2.85**	**−2.15**
small inducible cytokine subfamily A (Cys-Cys), member 17	SCYA17	−0.70	**−2.83**	−1.41
tumor protein p53 (Li-Fraumeni syndrome)	TP53	−1.07	**−2.75**	**−2.60**
fibroblast growth factor receptor 3	FGFR3	1.22	**−2.71**	**−2.42**
ubiquitin specific protease 6 (Tre-2 oncogene)	USP6	−1.65	**−2.61**	−1.66
mitogen induced nuclear orphan receptor (MINOR)	NR4A3	0.32	**−2.56**	−1.88
erythropoietin	EPO	−0.63	**−2.53**	**−2.22**
small inducible cytokine subfamily B (Cys-X-Cys), member 14 (BRAK)	SCYB14	**2.18**	**−2.53**	−1.64
MAD (mothers against decapentaplegic, Drosophila) homolog 6	MADH6	−1.89	**−2.51**	−0.44
small inducible cytokine subfamily A (Cys-Cys), member 14; MIP-1 delta; HCC-1	SCYA14	−0.76	**−2.46**	−1.77
small inducible cytokine A5 (RANTES)	SCYA5	0.87	**−2.41**	−1.63
CCAAT/enhancer binding protein (C/EBP), delta	CEBPD	0.38	**−2.39**	−1.59
cyclin A2	CCNA2	−1.46	**−2.37**	−1.66
apoptotic protease activating factor	APAF1	−0.35	**−2.33**	−1.62
grancalcin	GCL	0.54	**−2.31**	−1.14
vimentin	VIM	−0.20	**−2.30**	**−2.82**
collagen, type III, alpha 1 (Ehlers-Danlos syndrome type IV, autosomal dominant)	COL3A1	−1.75	**−2.28**	−1.58
insulin-like growth factor binding protein 10	IGFBP10	−1.18	**−2.26**	−1.95
SHIP; inositol polyphosphate-5-phosphatase, 145 kD	INPP5D	−0.16	**−2.22**	−1.04
immediate early protein	ETR101	0.78	**−2.20**	−1.27
tumor necrosis factor receptor superfamily, member 1B; TRAIL receptor 2	TNFRSF1B	0.29	**−2.20**	**−3.23**
chemokine (C-X3-C) receptor 1	CX3CR1	0.35	**−2.20**	−1.75
tailless homolog (Drosophila)	TLX	1.17	**−2.19**	**−3.75**
heat shock 70 kD protein 1	HSPA1B	0.56	**−2.10**	−1.10
damage-specific DNA binding protein 1 (127 kD)	DDB1	0.13	**−2.06**	−1.72
EphA3	EPHA3	−1.81	**−2.04**	**−3.77**
retinol-binding protein 3, interstitial	RBP3	1.44	**−2.03**	−1.85
properdin P factor, complement	PFC	−0.61	**−2.01**	−1.34
chemokine (C-X-C motif), receptor 4; fusin	CXCR4	−0.05	**−2.00**	−1.29
eukaryotic initiation factor 4A-I	EIF4AI	0.11	1.82	**3.21**
interleukin 2 receptor, alpha	CD25	−0.23	1.29	**3.13**
platelet-derived growth factor receptor, beta polypeptide	PDGFRB	1.41	1.46	**3.02**
calmodulin 3 (phosphorylase kinase, delta)	CALM3	−0.25	1.37	**2.97**
TIA1 cytotoxic granule-associated RNA-binding protein-like 1	TIAL1	0.69	1.37	**2.78**

Table 2. Continued.

Genes	Abb.	Regulation profile and Z-ratio		
		HA	ANO	Zr
protein phosphatase 1, regulatory subunit 10	PPP1R10	0.83	1.00	**2.66**
lymphocyte antigen 64 (mouse) homolog, radioprotective, 105 kD	LY64	1.22	0.71	**2.58**
zinc finger protein ZNF49	ZNF49	1.21	1.74	**2.57**
interferon regulatory factor 6	IRF6	1.74	1.07	**2.55**
major histocompatibility complex, class I, A	HLA-A	0.32	0.69	**2.48**
major histocompatibility complex, class II, DQ beta 1	HLA-DQB1	0.44	0.46	**2.40**
ubiquinol-cytochrome c reductase, Rieske iron-sulfur polypeptide-like 1	UQCRFSL1	−0.50	0.79	**2.31**
catenin (cadherin-associated protein), beta 1 (88 kD)	CTNNB1	0.56	1.00	**2.30**
bone morphogenetic protein 2	BMP2	0.35	1.49	**2.19**
villin2	VIL2	0.82	0.38	**2.18**
GDF-1 embryonic growth factor; cosmid R33485 containing pNORF1	GDF1	−0.21	1.19	**2.15**
primase, polypeptide 2A (58 kD)	PRIM2A	1.63	0.57	**2.14**
phosphogluconate dehydrogenase	PGD	−0.41	1.45	**2.06**
suppressor of Ty (S.cerevisiae) 4 homolog 1	SUPT4H1	0.44	0.98	**2.02**
apoptosis-associated tyrosine kinase	AATK	−1.66	−0.72	**−3.89**
anti-Mullerian hormone receptor, type II	AMHR2	0.20	−0.81	**−3.41**
ribosomal protein L7a; SURF3	RPL7A	−0.60	−1.41	**−3.15**
platelet-activating factor receptor	PTAFR	0.72	−1.48	**−2.88**
transcription elongation factor S-II, hS-II-T1	TEFS2	0.72	−1.53	**−2.74**
neuronal thread protein AD7c-NTP	AD7CNTP	1.24	−0.52	**−2.70**
ferritin, heavy polypeptide 1	FTH1	0.93	−1.10	**−2.67**
nuclear factor of kappa light polypeptide gene enhancer in B-cells inhibitor, epsilon	NFKBIE	1.08	−0.46	**−2.61**
major histocompatibility complex, class II, DN alpha	HLA-DNA	−0.11	−1.85	**−2.49**
POU domain, class 2, associating factor 1	POU2AF1	1.35	−1.49	**−2.45**
CAMP responsive element binding protein 1	CREB1	1.33	0.66	**−2.38**
polo (Drosophia)-like kinase	PLK	0.04	−1.80	**−2.34**
death effector domain-containing protein	DEDD	−1.29	−0.59	**−2.25**
interleukin 9 receptor	IL9R	−0.46	−1.33	**−2.24**
interleukin 9	IL9	1.02	0.75	**−2.22**
interferon-inducible	1-8D	−0.35	−0.78	**−2.19**
complement component 5 receptor 1 (C5a ligand)	C5R1	0.01	0.23	**−2.15**
hepatocyte growth factor (hepapoietin A; scatter factor)	HGF	−0.99	−1.88	**−2.14**

BMP2 on Zr surfaces.

The FGFR (fibroblast growth factor receptor) family members include FGFR3. The extracellular portion of the protein interacts with FGF, setting in motion a cascade of downstream signals, ultimately influencing mitogenesis and differentiation. This particular family member binds acidic and basic FGF hormone and plays a role in bone development and maintenance. FGF was combined with BMP, FGF prevented the differentiating action of BMP. The FGF was loosely bound to the matrix. Also, FGF signaling inhibited expression of alkaline phosphatase (ALKP) and blocked mineralization in osteoblastic cells[24]. In our study FGFR3 and FGF12 were down-regulated in cultures grown on Ano and Zr.

Normal bone function is assured when there is equilibrium between bone formation and bone re-sorption. Apoptosis, or programmed cell death, is characterized by the activation of cystein proteases called caspases, which cleave proteins essential for the survival of the cell. A member of this family, caspase1, has been identified by its ability to prote-olytically cleave and activate the inactive precursor of interlukin1, a cytokine involved in the processes such as inflammation, septic shock, and wound healing. This gene has been shown to induce cell apoptosis and may function in various developmental stages[10]. We founded the Ano and Zr Ti induced apoptosis in osteoblasts in our *in vitro* model system, and caspase-1 was involved in this process. The increased susceptitility to apoptosis of the less mature osteoblast could have important consequenese for bone remodeling.

In our experiment, we observed several genes relat-

ed with signal transduction for bone formation. However the expression of these genes such as MAPK13, MAP2K1, G protein coupled receptor 37, and G protein coupled receptor 9 were different according to different-coatings on Ti surfaces. MAPK13 and MAP2K1 have a member of the kinase family. MAP kinases act as an integration point for multiple biochemical signals and are involved in a wide variety of cellular processes such as proliferation, differentiation, transcription regulation and development[12,17,24]. In our experiment, we noted the down-regulation of MAPK13 and MAP2K1 on HA surfaces. CD183 is a G protein-coupled receptor with selectivity for three chemokines, termed IP10, Mig and I-TAC. IP10, Mig and I-TAC belong to the structural subfamily of CXC chemokines, in which a single amino acid residue separates the first two of four highly conserved Cys residues. Historically, CD183 is the third CXC chemokine receptor discovered and, therefore, commonly designated as CXCR3. Binding of chemokines to CD183 induces cellular responses that are involved in leukocyte traffic, most notably integrin activation, cytoskeletal changes and chemotactic migration. Inhibition by Bordetella pertussis toxin suggests that heterotrimeric G protein of the Gi-subclass couple to CD183. Signal transduction has not been further analyzed but may include the same enzymes that were identified in the signaling cascade induced by other chemokine receptors. As a consequence of chemokine-induced cellular desensitization (phosphorylation-dependent receptor internalization), cellular responses are typically rapid and short in duration. Cellular responsiveness is restored after dephosphorylation of intracellular receptors and subsequent recycling to the cell surface. A hallmark of CD183 is its prominent expression in vitro cultured effector/memory T cells, and in T cells present in many types of inflamed tissues. In addition, IP10, Mig and I-TAC are commonly produced by local cells in inflammatory lesion, suggesting that CD183 and its chemokines participate in the recruitment of inflammatory cells[17]. In our experiment, we noted the down-regulation of G protein coupled receptor 37 on Ano and Zr surfaces, and a down-regulation of G protein coupled receptor 9 on Ano and Zr surfaces.

We demonstrated that different-coatings on Ti surfaces were capable of modulating the expressions of some genes. Our results indicated that the gene encoding bone formation-related proteins was up-regulated mainly in the HA and Zr cultures. Carinci et al.[20] reported that surface topography exerted influences on the frequency and amount of formed bone, and that mineralized products can be guided by the surface topography of the implant. It has also been determined that bone formation induced by osteoblast-like cells at the implant-cell interface is quite a complex process, and involves a host of cellular functions, including cellular attachment, migration, and proliferation, followed by the expression of markers for osteoblast phenotype, and the synthesis, deposition, and mineralization of the bone matrix[25]. We believe that the data reported that the function of the signaling pathway in osteoblast differentiation may contribute to the identification of new therapeutics, for the treatment of poor bone quality. This study may provide dentists with a great deal of useful information for the improvement of present biomaterials, as well as the future development of new biomaterials.

Methods

Titanium Preparation

All Ti substrates were constructed from pure titaniums. The materials were Ti discs with a diameter of 10 mm, a thickness of 1 mm, in a coin-shaped circle. The Ti samples used in the experiments had different surfaces (control; non-coating on Ti, HA; Hydroxyapatite coating on Ti, Ano; HA coating on anodized surface Ti, Zr; zirconium-coating on Ti). Zirconium was coated on titanium surface by using plasma spraying, and Niobium was coated on titanium surface by using Physical Vapour Deposited (PVD) type coatings by O.M.T. (Luebeck, Germany). Table 1 shows these surface properties. After surface preparation, these samples were washed with distilled water, and then rinsed thoroughly in 70% ethanol and absolute ethanol. Prior to cell culturing, the discs were sterilized by γ-rays.

Cell Culture

MG63 cells were cultured on dental materials with different surfaces (control, HA, Ano, and Zr). The MG63 cells (KCLB© Korean Cell Line Bank) were cultured in (Dulbecco Eagle's minimum essential medium, Biowhittaker, Belgium) MEM medium with 10% fetal bovine serum, and antibiotics (Penicillin 100 U/mL and Streptomycin 100 μg/mL, Invitrogen, Milano, Italy) were seeded at 1×10^4/mL in a humidified atmosphere of 5% CO_2 at 37°C. These materials were placed in a 24-multiwell plate (NUNC^{TM}, Denmark). 1 mL of cell suspension was applied carefully to a 24-multiwell and the cells had been allowed to attach for 3 days to the MG63.

Scanning Electron Microscopy (SEM)

SEM (S-4700, HITACHI, Tokyo, Japan) was em-

ployed in order to determine the morphological cha-
racteristics of cells in culture. The advantages asso-
ciated with SEM include its large depth of focus, high
lateral resolution down to the nanometer range, the
feasibility to study structures with high aspect ratios,
and the direct production of surface images.

Human cDNA Microarray

A MG63 cDNA microarray was derived principally
from a commercially available master set of appro-
ximately 15,000 human verified-sequences (Research
Genetics, Inc., Huntsville, AL). The 15,000 human
cDNA clone set was sorted for a list of genes (1,152
elements) representing families such as differen-
tiation, development, proliferation, transformation,
cell cycle progression, immune response, transcrip-
tion and translation factors, oncogenes, and mole-
cules involved in cell growth and maintenance. PCR-
amplified cDNAs were spotted on nylon membranes.
The general methodology of arraying is based on the
procedures of DeRisi et al.[26].

RNA Preparation and cDNA Radiolabeling

The RNA was isolated from cultured cells which
adhered to the retrieved implants of different surfaces
(control, HA, Ano, and Zr) with Trizol (Invitrogen,
Milano, Italy). RNA was quantified via UV spectro-
photometry (spectrophotometer-DU650; Beckman,
Somerset, NJ, USA). After quantification, 3-10 μg of
total RNAs prepared from the MG63-treated dental
materials with different surfaces (control, HA, Ano,
and Zr) were used for each sample for adjustment of
different cell numbers. To synthesize ^{33}P-labeled
cDNAs, quantified RNA were labeled in a reverse
transcription reaction containing 5X first strand PCR
buffer, 1 μg of 24-mer poly dT primer, 4 μL of 20
mM each dNTP excluding dCTP, 4 μL of 0.1 M DTT,
40 U of RNase inhibitor, 6 μL of 3000 Ci/mmol a-^{33}P
dCTP to a final volume of 40 μL. The mixture was
heated at 65°C for 5 min, followed by incubation at
42°C for 3 min. Two μL (specific activity: 200,000
U/mL) of Superscript II reverse transcriptase (Invitro-
gen, Milano, Italy) was then added and the samples
were incubated for 30 min at 42°C, followed by the
addition of 2 μL of Superscript II reverse transcrip-
tase and another 30 min of incubation. Five μL of 0.5
M EDTA was added to chelate divalent cations. After
the addition of 10 μL of 0.1 M NaOH, the samples
were incubated at 65°C for 30 min to hydrolyze
remaining RNA. Following the addition of 25 μL of 1
M Tris (pH 8.0), the samples were purified using Bio-
Rad 6 purification columns (Hercules, CA, USA).
This resulted in 5×10^6 to 3×10^7 cpm per reaction[27].

Hybridization and Scanning

DNA microarrays were pre-hybridized in hybridi-
zation buffer containing 4.0 mL Microhyb (Invitrogen,
Milano, Italy), 10 μL of 10 mg/mL human Cot 1
DNA (Invitrogen, Milano, Italy), and 10 μL of 8
mg/mL poly dA (Pharmacia, Peapack, NJ). Both Cot
1 and poly dA were denatured at 95°C for 5 min prior
to use. After 4 h of pre-hybridization at 42°C, appro-
ximately 10^7 cpm/mL of heat-denatured (95°C, 5 min)
probes were added and incubation continued for 17 h
at 42°C. Hybridized arrays were washed three times
in 2X SSC and 0.1% SDS for 15 min at room tem-
perature. The microarrays were exposed to phosph-
orimager screens for 1-5 days, and the screens were
then scanned in a FLA-8000 (Fuji Photo Film Co.,
Japan) at 50 μm resolution[27,28].

Data Analysis

Microarray images were trimmed and rotated for
further analysis using L-Processor system (Fuji Photo
Film Co., Japan). Gene expression of each microar-
ray was captured by the intensity of each spot pro-
duced by radioactive isotopes. Pixels per spot were
counted by Arraygauge (Fuji Photo Film Co., Japan)
and exported to Microsoft Excel (Microsoft, Seattle,
WA, USA). The data were normalized with Z trans-
formation to obtain Z scores by subtracting each
average of gene intensity and dividing with each
standard deviation. Z scores provide each of 2,304
spots (two sets of 1,152 genes) genes with the dis-
tance from the average intensity and were expressed
in units of standard deviation. Thus, each Z score
provides flexibility to compare different sets of mic-
roarray experiments, by adjusting differences in hy-
bridization intensities. Gene expression difference as
compared with untreated control cells were calculat-
ed by comprising Z score differences (Z differences)
among the same genes. This facilitates comparing
each gene that had been up- or downregulated as
compared with the control cells. Z differences were
calculated first by subtracting Z scores of the controls
from each Z score of the sample. These differences
were normalized again to distribute their position by
subtracting the average Z difference and dividing
with the standard deviation of the Z differences. These
distributions represent the Z ratio value and provide
the efficiency for comparing each microarray experi-
ment[27]. Scatter plots of intensity values were produc-
ed by Spotfire (Spotfire, Inc., Cambridge, MA)[29].
Cluster analysis was performed on the Z-transformed
microarray data by using two programs available as
shareware from Michael Eisen's laboratory (http://
rana.lbl.gov). Clustering of changes in gene expres-
sion was determined by using a public domain clu-

ster based on pair wise complete-linkage cluster analysis[30].

Acknowledgements

References

1. Shah, A. K. *et al*. High-resolution morphometric analysis of human osteoblastic cell adhesion on clinically relevant orthopedic alloys. *Bone* **24**(5):499-506 (1999).

2. Cooper, L. F. *et al*. Incipient analysis of mesenchymal stem-cell-derived osteogenesis. *J. Dent. Res.* **80**(1):314-320 (2001).

3. Carinci, F. *et al*. Titanium-cell interaction: analysis of gene expression profiling. *J. Biomed. Mater. Res.* **66B**(1):341-346 (2003).

4. Viornery, C. *et al*. Osteoblast culture on polished titanium disks modified with phosphonic acids. *J. Biomed. Mater. Res.* **62**(1):149-155 (2002).

5. Kim, H. K., Jang, J. W. & Lee, C. H. Surface modification of implant materials and its effect on attachment and proliferation of bone cells. *J. Mater. Sci. Mater. Med.* **15**(7):825-830 (2004).

6. Ogawa, T., Sukotjo, C. & Nishimura, I. Modulated bone matrix-related gene expression is associated with differences in interfacial strength of different implant surface roughness. *J. Prosthodont.* **11**(4): 241-247 (2002).

7. Schneider, G. B. *et al*. Implant surface roughness affects osteoblast gene expression. *J. Dent. Res.* **82**(5): 372-376 (2003).

8. Carinci, F. *et al*. Zirconium oxide: analysis of MG63 osteoblast-like cell response by means of a microarray technology. *Biomaterials* **25**(2):215-228 (2004).

9. Orsini, G. *et al*. Surface analysis of machined versus sandblasted and acid-etched titanium implants. *Int. J. Oral. Maxillofac. Implants* **15**(6):779-784 (2000).

10. Son, W. W. *et al*. *In vivo* histological response to anodized and anodized/hydrothermally treated titanium implants. *J. Biomed. Mater. Res. B. Appl. Biomater.* **66**(2):520-525 (2003).

11. Ogawa, T. & Nishimura, I. Different bone integration profiles of turned and acid-etched implants associated with modulated expression of extracellular matrix genes. *Int. J. Oral Maxillofac. Implant* **18**(2):200-210 (2003).

12. Kim, C. S. *et al*. Effect of various implant coatings on biological responses in MG63 using cDNA microarray. *J. Oral Rehabil.* **33**:368-379 (2006)

13. Kim, C. S. *et al*. Gene-expression profiling of titanium-cell interaction. *J. Korea Acad. Prosthdont.* **43**(3): 393-408 (2005).

14. Sohn, S. H. *et al*. Biological responses in osteoblast-like cell line accoding to thin layer hydroxyapatite coatings on anodized titanium. *J. Oral Rehabil.* **33**: 898-911 (2006).

15. Sohn, S. H. *et al*. Biological effects of different thin layer hydroxyapatite coatings on anodized titanium. *Mol. Cell. Toxicol.* **1**(4):237-247 (2005).

16. Sohn, S. H. *et al*. Biological effects of Ceramic-coating on titanium. *Mol. Cell. Toxicol.* **2**(2):97-105 (2006).

17. Carinci, F. *et al*. Analysis of osteoblast-like MG63 cells' response to a rough implant surface by means of DNA microarray. *J. Oral Implantol.* **29**(5):215-220 (2003).

18. Hornez, J. C. *et al*. Multiple parameter cytotoxicity index on dental alloys and pure metals. *Biomol. Eng.* **19**(2-6):103-117 (2002).

19. Monsees, T. K. *et al*. Effects of different titanium alloys and nanosize surface patterning on adhesion, differentiation, and orientation of osteoblast-like cells. *Cells Tissues Organs* **180**(2):81-95 (2005).

20. Carinci, F. *et al*. Analysis of MG63 osteoblastic-cell response to a new nanoporous implant surface by means of a microarray technology. *Clin. Oral Implants Res.* **15**(2):180-186 (2004).

21. Lossdorfer, S. *et al*. Microrough implant surface topographies increase osteogenesis by reducing osteoclast formation and activity. *J. Biomed. Mater. Res.* **70A**(3):361-369 (2004).

22. Wang, E. A. *et al*. Purification and characterization of other distinct bone-inducing factors. *Proc. Natl. Acad. Sci. USA.* **85**:9484-9488 (1988).

23. Reddi, A. H. *et al*. Bone morphogenetic proteins: an unconventional approach to isolation of first mammalian morphogens. *Cytokine Growth Factor Rev.* **8**: 11-20 (1997).

24. Chaudhary, L. R. Hofmeister, A. M. & Hruska, K. A. Differential growth factor control of bone formation through osteoprogenitor differentiation. *Bone* **34**(3):

402-411 (2004).

25. Mustafa, K. *et al*. Determining optimal surface roughness of TiO (2) blasted titanium implant material for attachment, proliferation and differentiation of cells derived from human mandibular alveolar bone. *Clin. Oral Implants Res.* **12**(5):515-525 (2001).

26. DeRisi, J. *et al*. Use of a cDNA microarray to analyse gene expression patterns in human cancer. *Nat. Genet.* **14**(4):457-460 (1996).

27. Vawter, M. P. *et al*. Application of cDNA microarrays to examine gene expression differences in schizophrenia. *Brain Res. Bull.* **55**(5):641-650 (2001).

28. Park, G. H. *et al*. Genome-wide expression profiling of 8-chloroadenosine- and 8-chloro-cAMP-treated human neuroblastoma cells using radioactive human cDNA microarray. *Exp. Mol. Med.* **34**(3):184-193 (2002).

29. Tanaka, T. S. *et al*. Genome-wide expression profiling of mid-gestation placenta and embryo using a 15,000 mouse developmental cDNA microarray. *Proc. Natl. Acad. Sci. USA.* **97**(16):9127-9132 (2000).

30. Eisen, M. B. *et al*. Cluster analysis and display of genome-wide expression patterns. *Proc. Natl. Acad. Sci. USA.* **95**(25):14863-14868 (1998).